

Temperature Dependence of the Spin State of a Co^{3+} Ion in $R\text{CoO}_3$ ($R = \text{La}, \text{Gd}$) Cobaltites

R. Yu. Babkin^a, K. V. Lamonova^a, S. M. Orel^a, S. G. Ovchinnikov^{b, *}, and Yu. G. Pashkevich^a

^a Donetsk Institute for Physics and Engineering, National Academy of Sciences of Ukraine, Donetsk, 83114 Ukraine

^b Kirensky Institute of Physics, Siberian Branch, Russian Academy of Sciences, Akademgorodok, Krasnoyarsk, 660036 Russia

* e-mail: sgo@iph.krasn.ru

Received March 24, 2014

Changes in the spin state of Co^{3+} ions in LaCoO_3 and GdCoO_3 compounds are studied through the use of the temperature dependence of the magnetic susceptibility and the modified crystal field theory. It is shown that the spin subsystem of Co^{3+} ions in LaCoO_3 and GdCoO_3 undergoes the spin-crossover type transition between the high-spin ($S = 2$) and low-spin ($S = 0$) states without any contribution of the intermediate-spin state ($S = 1$).

DOI: 10.1134/S0021364014080037

1. INTRODUCTION

Rare-earth cobaltites $R\text{CoO}_3$ (where R is a rare-earth element) with the perovskite type structure belong to a vast class of compounds with strongly correlated electrons and the competition between different spin states [1]. The intimate coupling between structural and spin degrees of freedom makes it possible not only to control spin and magnetic subsystems but also to change the transport characteristics of $R\text{CoO}_3$ by varying the temperature and applying pressure, light, and a magnetic field. In particular, the unusual behavior of the temperature dependence of the magnetic susceptibility [2, 3] suggests that LaCoO_3 undergoes two phase transitions. One of them is related to the change in the spin state of Co^{3+} ion, whereas the other transition manifests itself in changes in the transport characteristics (metal–insulator transition). The nature and characteristic features of the spin-state transition are still under discussion. Indeed, the electronic configuration of trivalent cobalt ($3d^6$) implies the existence of three spin states: the low-spin (LS) state ($S = 0$), the intermediate-spin (IS) state ($S = 1$), and the high-spin (HS) state ($S = 2$). On the one hand, it is not quite clear whether the spin-state transition is the classical LS \longleftrightarrow HS spin crossover [4] or it obeys a more complicated scenario involving the intermediate-spin state, LS \longleftrightarrow IS \longleftrightarrow HS [5]. On the other hand, the nature of the spin-state transition still remains a topical problem. One may wonder whether this transition results from the thermally induced occupation of the energy levels corresponding to the different spin states or the temperature leads to the rearrangement of the set of energy levels in such a way

that the ground and excited spin states exchange their roles. Is it possible that both mechanisms simultaneously contribute to the transition?

Our work aims at the study of the characteristic features and of the nature of the spin-state transitions induced by temperature in $R\text{CoO}_3$ compounds with $R = \text{La}$ and Gd . For the calculations and the further analysis, we use the crystallographic data for LaCoO_3 [6] and GdCoO_3 [7], as well as the semiempirical theory of the modified crystal field, which was described in detail in [8]. The essence of this theory can be formulated as follows.

(i) Similarly to the classical crystal field theory, we assume that the crystal potential is created by the electron and nuclear charges surrounding a paramagnetic ion and forming the coordination complex.

(ii) All calculations are performed in the single-configuration approximation. In this case, the set of basis functions corresponding to a specified electron configuration includes a finite number of orthonormal antisymmetric multielectron wavefunctions.

(iii) The multielectron wavefunctions are constructed using the single-electron hydrogen-like functions corresponding to the effective nuclear charge Z_{eff} , which is considered as a variational parameter.

(iv) In the Born–Oppenheimer approximation, the eigenfunctions used to construct a solution are parametrically dependent on the positions and charges of ligands.

(v) The relativistic spin–orbit interaction and the interaction with the applied magnetic field are taken into account.

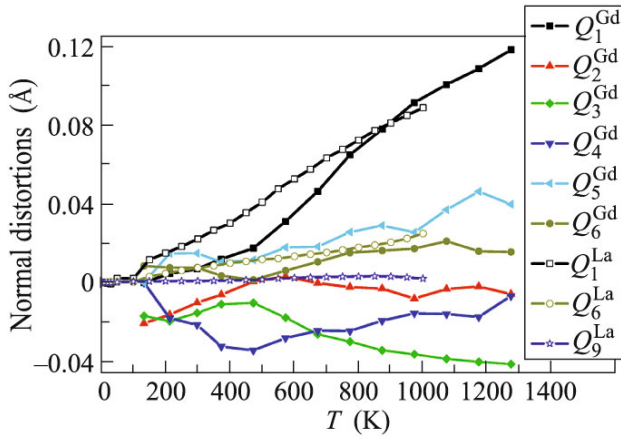


Fig. 1. (Color online) Temperature dependence of the $Q_i^{\text{La(Gd)}}$ distortions of the octahedral complex with Co^{3+} ion in LaCoO_3 and GdCoO_3 compounds. The vertical axis represents the displacements of ligands $\Delta\xi_j$ ($\xi = x, y, z; j = 1, 2, \dots, N; N$ is the number of ligands in the coordination complex). The normal displacements Q_α ($\alpha = 1, 2, \dots, 3N - 3$) are linear combinations of $\Delta\xi_j$ [10].

2. ANALYSIS OF THE DISTORTIONS AND CALCULATIONS OF THE ENERGY AND MAGNETIC SUSCEPTIBILITY

The crystal structure of $R\text{CoO}_3$ compounds with $R = \text{La}$ and Gd is well known [9]. Here, we only note that Co^{3+} ions occupy the same crystallographic position. They are located within distorted oxygen octahedra with the parameters (cobalt–oxygen bond lengths and angles) depending on the temperature. The temperature dependences for the most significant octahedral distortions classified using the formalism of normal coordinates [10] are shown in Fig. 1.

LaCoO₃ cobaltite. For LaCoO_3 , it is clear that the most significant distortion is the homogeneous expansion described by the normal coordinate Q_1^{La} (so-called breathing mode) (see Fig. 1). With the growth of temperature, Q_1^{La} increases; i.e., the volume of the coordination complexes increases. The $Q_1^{\text{La}}(T)$ curve for LaCoO_3 (Fig. 1a) exhibits features near 100 and 550 K. It is important that, just at the same temperatures, the magnetic susceptibility also exhibits an anomalous behavior [2, 3] (Fig. 2). Note also that the other types of distortions also arise in the complexes; however, they vary with temperature only slightly and do not produce a decisive effect on the temperature evolution of the spin subsystem in LaCoO_3 .

Using the structural data and the technique for calculation of magnetic characteristics applicable for these compounds and described in detail in [11], we calculated the free energy, magnetization, and magnetic susceptibility for the cobalt subsystem in LaCoO_3 as functions of temperature and the effective nuclear charge $Z_{\text{eff}}^{\text{Co}^{3+}}$ of cobalt ions. (Note that, in contrast to the conventional crystal field theory, which deals with the effective nuclear charge $Z_{\text{eff}}^{\text{FI}}$ of a *free ion*, the modified crystal field theory uses the effective nuclear charge of an ion placed into the *crystal field*, $Z_{\text{eff}}^{\text{CF}} = Z_{\text{eff}}^{\text{FI}} - \sigma^{\text{CF}}$ (where σ^{CF} characterizes the additional screening related to the crystal field). The parameter σ^{CF} depends on the nature, arrangement, and number of ligands; hence, $Z_{\text{eff}}^{\text{CF}}$ also depends on the characteristics of the crystal field rather than being a fixed number.) In the modified crystal field theory,

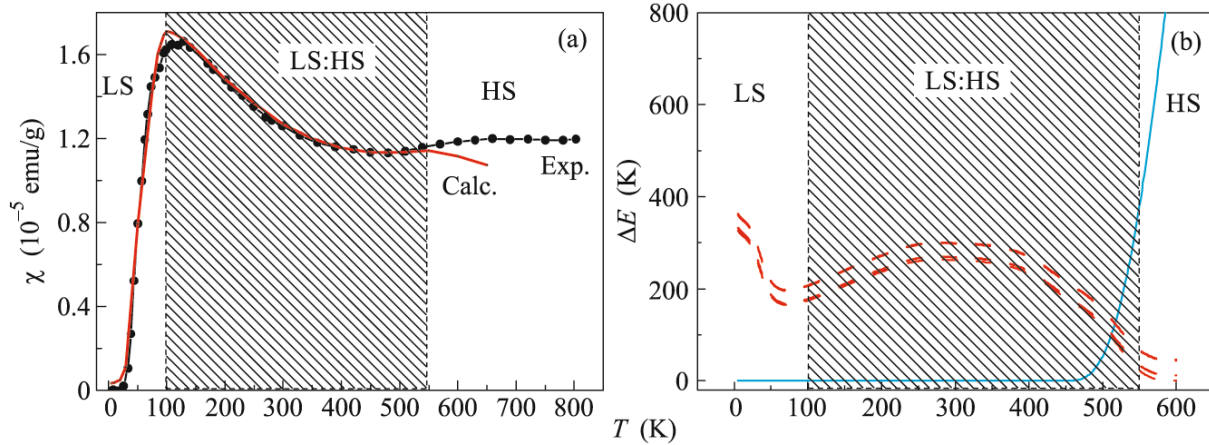


Fig. 2. (Color online) (a) Temperature dependence of the magnetic susceptibility. The calculations are shown by the solid line and the experimental data are denoted by circles. (b) Temperature dependence of the first six energy levels of the Co^{3+} ion in LaCoO_3 . The solid blue curve corresponds to spin $S = 0$ and the dashed red curves correspond to spin $S = 2$. The energy is measured from the ground state.

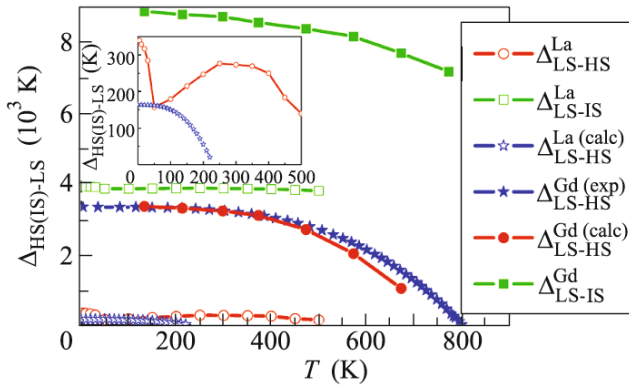


Fig. 3. (Color online) Temperature dependence of the $\Delta_{\text{HS}(1\text{S})\text{-LS}}(T) = E_{\text{HS}(1\text{S})} - E_{\text{LS}}$ spin gaps in LaCoO_3 and GdCoO_3 compounds.

$Z_{\text{eff}}^{\text{CF}}$ is a parameter controlling the system, which is generally speaking unknown since it depends on the properties of the specific host crystal and thus on the temperature dependence of the parameters characterizing the given coordination complex. In the framework of modified crystal field theory, we need to have additional experimental data to determine this parameter. In some cases, the corresponding experimental data are provided by the values of the g -factor measured using the electron spin resonance (ESR) spectroscopy [12].

In Fig. 2a, we demonstrate the measured and calculated temperature dependence of the magnetic susceptibility. We see that the calculated curve fits well the experimental data up to a temperature of about 550 K. At higher temperatures, the discrepancy between these two curves can result from the transition to the metallic phase [13], which falls beyond the range of applicability of the modified crystal field theory.

In Fig 2b, we illustrate the temperature evolution of six lower energy levels in Co^{3+} ion. In the vicinity of 550 K, there occurs a crossover from the low-spin state to the high-spin state. As a result, we have an $\text{LS} \leftrightarrow \text{HS}$ spin-state transition. It is clear that the energies of excited levels at $T \leq 200$ K are $\Delta E \geq 200$ K; i.e., the energy levels corresponding to the high-spin state are either completely empty or nearly unoccupied within this temperature range. Thus, Co^{3+} ions correspond to the nonmagnetic state with $S = 0$. At temperatures above 200 K, the energies of excited levels are comparable to kT . This ensures the possibility of their thermally induced filling. Therefore, within this temperature range, the main contribution to the susceptibility comes from the excited high-spin states (the hatched area in Fig. 2); nevertheless, the ground state is still the low-spin state. Finally, at $T \geq 550$ K, there appears a spin-crossover transition and the ground state becomes magnetic with spin $S = 2$.

Note that the intermediate-spin states correspond to significantly higher energies. This conclusion is supported by the calculations of spin gaps represented in Fig. 3. Here, the spin gap is defined as the difference between the energy levels corresponding to two different spin states. We see that, in the temperature range under study, the spin gap $\Delta_{\text{IS-LS}}^{\text{La}}(T) = E_{\text{IS}} - E_{\text{LS}}$ far exceeds $\Delta_{\text{HS-LS}}^{\text{La}}(T) = E_{\text{HS}} - E_{\text{LS}}$. Hence, the intermediate spin states hardly affect the characteristics of the spin-state transition.

In addition, the calculations demonstrate (see inset in Fig. 3) that the temperature dependence of the spin gap $\Delta_{\text{HS-LS}}^{\text{La}}(T)$ behaves nonmonotonically in contrast to $\Delta_{\text{HS-LS}}^{\text{Gd}}(T)$ [7], and the values of $\Delta_{\text{HS-LS}}^{\text{La}}(T)$ appreciably differ from the estimates reported in [14].

To analyze the evolution of the spin subsystem in the $[\text{CoO}_6]$ octahedral complex, which is the main structural block of the LaCoO_3 compound, we constructed the diagram of spin states (spin-state diagram), Fig. 4. The technique used to construct spin-state diagrams is described in detail in [15]. Taking into account the temperature dependence of the crystallographic parameters of the LaCoO_3 compound, we can conclude that the spin-state diagram is the surface with the average spin squared for a paramagnetic ion $\langle S^2 \rangle = S(S + 1)$ drawn in the plane of the temperature and the effective nuclear charge of a cobalt ion. We see that, in the temperature range under study for $Z_{\text{eff}}^{\text{Co}^{3+}}$, the ground state can correspond to only either the low-spin or high-spin states. The ranges corresponding to the intermediate spin states do not appear since the trigonal distortions of Q_4 , Q_5 , and Q_6 types in the system (see Fig. 1) are an order of magnitude smaller than those that can stabilize the states with spin $S = 1$ [8]. In Fig. 4, we see a narrow region that looks like a range of intermediate-spin states. In this case, it is related to the effects of visualization of the results of calculations. Actually, the weight of the intermediate-spin states in this crossover region is as small as over the whole spin diagram. Comparing the results of the calculations of $\chi(T, Z_{\text{eff}}^{\text{Co}^{3+}})$ with the experimental $\chi_{\text{exp}}(T)$ curve (Fig. 2a), we reconstructed the temperature dependence $Z_{\text{eff}}^{\text{Co}^{3+}}(T)$ (marked in green in Fig. 4), i.e., the trajectory of changes in the state of the spin subsystem corresponding to Co^{3+} ion.

The nontrivial behavior of the $Z_{\text{eff}}^{\text{Co}^{3+}}(T)$ curve in Fig. 4 explains the unusual ‘‘prolonged’’ spin-state transition observed in LaCoO_3 . An abrupt change in the direction of the curve near 50 K, its subsequent long run along the boundary, and, finally, another abrupt turn in the vicinity of 500 K toward the high-

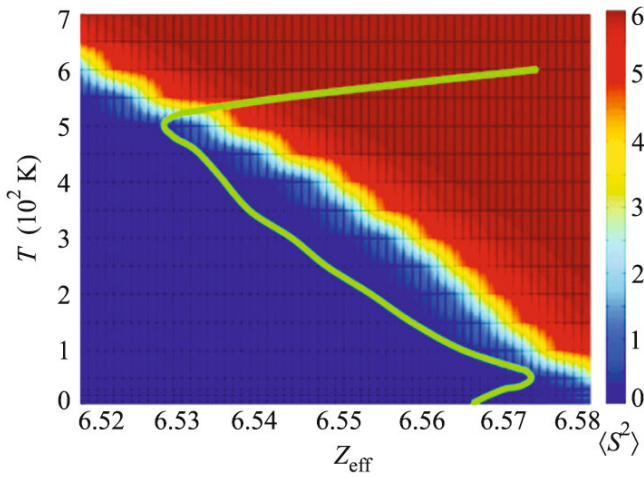


Fig. 4. (Color online) Spin-state diagram for the Co^{3+} ion in LaCoO_3 . The green curve corresponds to the temperature dependence of the effective charge $Z_{\text{eff}}^{\text{Co}^{3+}}(T)$.

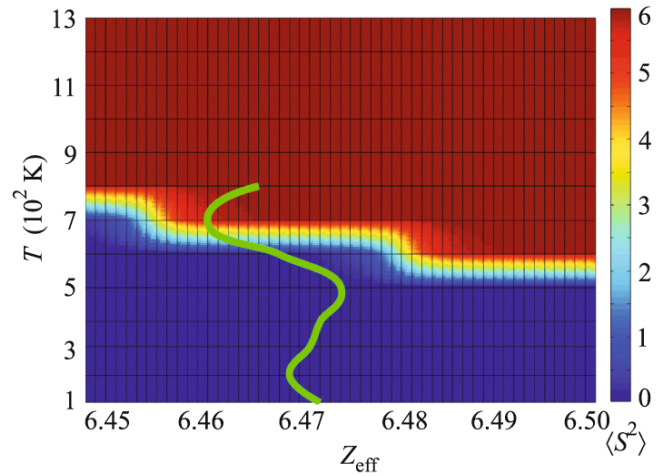


Fig. 5. (Color online) Spin-state diagram for Co^{3+} ion in GdCoO_3 . The green curve corresponds to the temperature dependence of the effective charge $Z_{\text{eff}}^{\text{Co}^{3+}}(T)$.

spin state indicate the actual realization of the $\text{LS} \leftrightarrow \text{HS}$ spin-state transition. Thus, the suggestion that the transition in LaCoO_3 occurs involving the intermediate-spin states seems to be unjustified.

Let us note in conclusion that the effective nuclear charge for the Co^{3+} ion located in the host LaCoO_3 crystal decreases by about 20% in comparison to that for the free trivalent cobalt ion ($Z_{\text{eff}}^{\text{FI}}(\text{Co}^{3+}) = 8.3$) [16]. Within the temperature range from 0 to 1000 K, the effective nuclear charge varies from 6.53 to 6.57. In other words, the temperature-induced distortions of the octahedral complex lead to the lowering of $Z_{\text{eff}}^{\text{Co}^{3+}}(T)$ by less than 1%. In spite of that, the temperature-induced changes in $Z_{\text{eff}}^{\text{Co}^{3+}}(T)$ lead to an appreciable rearrangement of the energy levels accompanied by the change in the ground state.

GdCoO₃ cobaltite. To compare the conditions needed for the realization of the spin-state transition in LaCoO_3 and GdCoO_3 , we calculated the spin-state diagram for a Co^{3+} ion in the $[\text{CoO}_6]$ octahedral complex, which is the main structural block of the GdCoO_3 compound (Fig. 4). Here, the $[\text{CoO}_6]$ coordination complex is distorted more strongly than in LaCoO_3 (see Fig. 1); it includes the Jahn–Teller type distortions (Q_2^{Gd} and Q_3^{Gd}), whereas the trigonal distortions (Q_4^{Gd} , Q_5^{Gd} , and Q_6^{Gd}) play a more significant role. Both of these distortion types can favor the realization of the intermediate-spin states under the condition that the displacements of ligands are as large as 0.2 Å. Actually, the displacements of ligands do not exceed 0.04 Å. Therefore, as in the case of LaCoO_3 , the intermediate-spin states (see Fig. 3) do not affect

the characteristics of the transition. A steep growth of $Q_1^{\text{Gd}}(T)$ in GdCoO_3 (see Fig. 1b) within the 300–700 K temperature range corresponds to the growth of inverse magnetic susceptibility [7].

In the spin-state diagram shown in Fig. 5, we show the trajectory illustrating the temperature-induced changes in the spin state. We can see that, in spite of its nonmonotonic behavior within the 100–800 K temperature range, the variation of the effective nuclear charge does not exceed 0.2%, and the spin-state transition in GdCoO_3 takes place at 650–700 K.

3. CONCLUSIONS

To summarize, we have studied the temperature dependence of the spin state of a Co^{3+} ion in LaCoO_3 and GdCoO_3 compounds using the temperature dependence of the magnetic susceptibility and of the structural X-ray diffraction data obtained in a wide temperature range, as well as the calculation technique based on the modified crystal field theory. The scenarios underlying the temperature behavior of Co^{3+} ions in LaCoO_3 and GdCoO_3 are described.

It is found that a Co^{3+} ion in LaCoO_3 is in the state with $S = 0$ up to 150 K and in the state with spin $S = 2$ above 550 K. In the intermediate temperature range $150 \text{ K} \leq T \leq 550 \text{ K}$, the magnetic susceptibility is formed by the temperature-induced filling of the excited high-spin states. The spin-state transition involves only two spin states, $\text{LS} \leftrightarrow \text{HS}$.

In GdCoO_3 , the cobalt subsystem is in the state with $S = 0$. The levels corresponding to the high-spin state begin to be occupied only at temperatures in the vicinity of 650–700 K. This is accompanied by the

rearrangement of the energy level system, resulting in the spin-state transition.

Finally, we can make the following general conclusion. The thermally induced spin-state transitions always take place owing to the simultaneous contribution of two factors: the thermal occupation of the levels corresponding to different spin states and the rearrangement of the energy level system, as a result of which the ground and excited spin states exchange their roles. Such rearrangement is related to the thermal expansion of the crystal lattice, which plays the role of negative pressure.

In both cases, the intermediate-spin state does not take part in the formation of the magnetic characteristics of the crystal, since its energy in the whole temperature range under study is much higher than those corresponding to high- and low-spin states.

This work was supported by the Russian–Ukrainian project no. 27-02-12, by the National Academy of Sciences of Ukraine (complex basic research project no. 91/14-N), by the Council of the President of the Russian Federation for Support of Young Scientists and Leading Scientific Schools (project no. NSh-2886.2014.2), by the Presidium of the Russian Academy of Sciences (project no. 216), and by the Russian Foundation of the Basic Research (project no. 13-02-00358).

REFERENCES

1. N. B. Ivanova, S. G. Ovchinnikov, M. M. Korshunov, I. M. Eremin, and N. V. Kazak, *Phys. Usp.* **52**, 789 (2009).
2. V. G. Bhide, D. S. Rajoria, G. R. Rao, and C. N. R. Rao, *Phys. Rev. B* **6**, 1021 (1972).
3. C. Zobel, M. Kriener, D. Bruns, J. Baier, M. Gruninger, and T. Lorenz, *Phys. Rev. B* **66**, 020402 (2002).
4. J. B. Goodenough, *J. Phys. Chem. Solids* **6**, 287 (1958).
5. R. H. Potze, G. A. Sawatzky, and M. Abbate, *Phys. Rev. B* **51**, 501 (1995).
6. P. G. Radaelli and S.-W. Cheong, *Phys. Rev. B* **66**, 094408 (2002).
7. Yu. S. Orlov, L. A. Solovyov, V. A. Dudnikov, A. S. Fedorov, A. A. Kuzubov, N. V. Kazak, V. N. Voronov, S. N. Vereshchagin, N. N. Shishkina, N. S. Perov, K. V. Lamonova, R. Yu. Babkin, Yu. G. Pashkevich, A. G. Anshits, and S. G. Ovchinnikov, *Phys. Rev. B* **88**, 235105 (2013).
8. K. V. Lamonova, E. S. Zhitlukhina, R. Yu. Babkin, S. M. Orel, S. G. Ovchinnikov, and Yu. G. Pashkevich, *J. Phys. Chem. A* **115**, 13596 (2011).
9. G. Thornton, B. C. Tofield, and A. W. Hewat, *J. Solid State Chem.* **61**, 301 (1986).
10. I. B. Bersuker, in *Electronic Structure and Properties of Transition Metal Compounds. Introduction to the Theory*, Ed. by I. B. Bersuker (Wiley, New York, 1996).
11. O. V. Gorostaeva, K. V. Lamonova, S. M. Orel, and Yu. G. Pashkevich, *J. Low Temp. Phys.* **39**, 343 (2013).
12. R. Yu. Babkin, K. V. Lamonova, S. M. Orel, Yu. G. Pashkevich, and V. F. Meshcheryakov, *Opt. Spectrosc.* **112**, 438 (2012).
13. J. Baier, S. Jodlauk, M. Kriener, A. Reichl, C. Zobel, H. Kierspel, A. Freimuth, and T. Lorenz, *Phys. Rev. B* **71**, 014443 (2005).
14. K. Knizek, Z. Jirak, J. Hejtmanek, M. Veverka, M. Marysko, G. Maris, and T. T. M. Palstra, *Eur. Phys. J. B* **47**, 213 (2005).
15. E. S. Zhitlukhina, K. V. Lamonova, S. M. Orel, and Yu. G. Pashkevich, *J. Low Temp. Phys.* **38**, 930 (2012).
16. R. Yu. Babkin, K. V. Lamonova, S. M. Orel, and Yu. G. Pashkevich, *Opt. Spectrosc.* **107**, 9 (2009).

Translated by K. Kugel